# NASA Technical Memorandum 81785

# NONLINEAR STATIC TPS ANALYSIS



Jerrold M. Housner
Ramon Garcia

March 1980

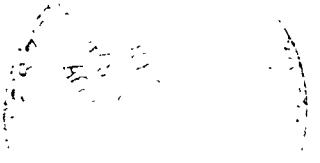

National Aeronautics and
Space Administration

**Langley Research Center**
Hampton Virginia 23665

# NONLINEAR STATIC TPS ANALYSIS

Jerrold M. Housner and Ramon Garcia
NASA Langley Research Center
Hampton, VA 23665

## SUMMARY

A nonlinear analysis which includes the effect of mismatch and filler bar has been developed to predict the SIP/RSI through-the-thickness interface stresses. The analysis assumes that the tile is rigid and that the SIP and filler bar behave as nonlinear spring foundations which are characterized by experimental stress-strain data. Interface stresses are calculated numerically from the tile equilibrium equations using a Newton iteration scheme.

Parametric studies were conducted using this analysis for simulated shock loading (combined load and moment) on square tiles. In addition, expected loads on an actual tile were also studied. The results of these studies indicate that when no mismatch is present, linear solutions tend to give nonconservative maximum stresses relative to the nonlinear solutions. When mismatch is present, the linear maximum stresses are only conservative at low load levels and highly nonconservative at high load levels. These studies also indicated that although the presence of filler bar reduces maximum tensile stresses in some cases, it does not appear that the nominal dimension filler bar, (1.27 cm or 1/2 inch wide) can reduce the nonlinear stress to a level at which the linear solution becomes conservative relative to the nonlinear solution. Moreover, on an outboard trailing edge elevon tile at descent with $+20^{\circ}$ flap, (tile 139), the linear analysis is 49% nonconservative relative to the nonlinear analysis with filler bar.

## INTRODUCTION

Tests performed by Rockwell International and Langley Research Center indicate that the SIP possesses a highly nonlinear stress-strain relationship. It is the purpose of this report to present an analysis to predict some of the possible consequences of the SIP nonlinearity on SIP/RSI interface through-the-thickness stresses. These stresses are considered since they appear to be critical to the integrity of the TPS. The application of this analysis to selected parametric studies is also presented and comparisons with a linear analysis are discussed.

## GOVERNING EQUATIONS

### Assumptions

Geometrical - In order to produce an efficient analysis applicable to a large number of tiles, SIP footprints and mismatch geometries, the following assumptions are made:

(a) The tile behaves as a rigid body.

(b) The tile rotations are small.

(c) There exists an inherent mismatch between the tile and the substrate structure which is due to tile imperfections, tile warpage, substrate initial curvature or substrate deformation under load.

Material - In order to account for the nonlinear SIP behavior observed experimentally, the following additional assumptions are made:

(d) The SIP behaves as a nonlinear continuous spring - type foundation.

(e) The stress strain relationship for the SIP may be accurately characterized as function of powers of the SIP strain.

### Equilibrium of Rigid Tile

Consider the tile geometry shown in figures 1a, b where P is a positive vertical load acting at x = xp and y = yp, and $M_x$ and $M_y$ are moments acting about the positive x and y axes respectively. Equilibrium of the tile results in

$$\sum_{j=1}^{2}\int_{A_j}\sigma_j\, dA_j - P = 0 \tag{1}$$

$$\sum_{j=1}^{2}\int_{A_j}\sigma_j\, y\, dA_j - M_x - Py_p = 0 \tag{2}$$

$$-\sum_{j=1}^{2}\int_{A_j}\sigma_j\, x\, dA_j - M_y + Px_p = 0 \tag{3}$$

where $A_1$ and $A_2$ are the portions of the tile bottom surface area supported by filler bar and SIP footprint respectively, and $\sigma_1$ and $\sigma_2$ are the SIP/RSI interface through-the-thickness stresses in the filler bar and SIP footprint respectively (positive stress causing extension of the SIP).

As a consequence of assumptions (d) and (e), the constitutive relationship for the SIP may be expressed as

$$\sigma_j = \begin{cases} \sum_{q=0}^{N_j} C_{T,qj} (\epsilon_j)^q & \text{for } \epsilon \geq 0 \\ \sum_{q=0}^{N_j} C_{C,qj} (\epsilon_j)^q & \text{for } \epsilon < 0 \end{cases} \tag{4}$$

where $C_{T,qj}$ and $C_{C,qj}$ are coefficients determined by experiment for the filler bar when $j = 1$ and for the SIP footprint when $j = 2$. Inasmuch as the filler bar is not bonded to the tile,

$$C_{T,q1} = 0 \tag{5}$$

Furthermore, as a consequence of assumption (a) - (c) and figure 1

$$W = W_o + y\alpha_x - x\alpha_y \tag{6}$$

$$\epsilon_j = (W - \bar{W}) / t_j \tag{7}$$

where $w$ is the local positive vertical tile displacement; $w_o$ is the tile displacement at $x = y = 0$; $\alpha_x$ and $\alpha_y$ are rotations about the x and y axes respectively (positive as shown in figure 1a); $\epsilon_1$ and $\epsilon_2$ are the filler bar and SIP through-the-thickness strains respectively; $t_1$ and $t_2$ are the SIP and filler bar thicknesses respectively and, $\bar{W}$ is given by

$$\bar{W} = W_S - W_I \tag{8}$$

in which $W_S$ is due to substrate deformation or mismatch and $W_I$ is due to tile imperfection or warpage.

Substituting eqs. (4), (6), (7), and (8) into eqs. (1) - (3) yields

$$\sum_{j=1}^{2} \left[ \int_{A_j} \sum_{q=0}^{N_j} \bar{C}_{qj} \left( W_o + y\alpha_x - x\alpha_y - W_S + W_I \right)^q dA_j \right] - P = 0 \tag{9}$$

$$\sum_{j=1}^{2} \left[ \int_{A_j} \sum_{q=0}^{N_j} y \bar{C}_{qj} \left( W_o + y\alpha_x - x\alpha_y - W_S + W_I \right)^q dA_j \right] - M_x - Py_p = 0 \tag{10}$$

$$-\sum_{j=1}^{2}\left[\int\sum_{q=0}^{4} x\,\bar{C}_{qj}\left(W_o + y\alpha_x - x\alpha_y - w_s + w_I\right)^q dA_j\right] - M_y + Px_p = 0 \qquad (11)$$

where

$$\bar{C}_{qj} = \begin{cases} C_{T,qj}/t_j^q & \text{for } \epsilon \geq 0 \\ C_{c,qj}/t_j^q & \text{for } \epsilon < 0 \end{cases} \qquad (12)$$

## Solution Procedure

Equations (9) - (11) may be solved for the three degrees of freedom, ( $W_o, \alpha_x, \alpha_y$ ), using a Newton iteration procedure. Thus the approximation to the solution vector is given by

$$\begin{vmatrix} W_o \\ \alpha_x \\ \alpha_y \end{vmatrix}_{(i+1)} = \begin{vmatrix} W_o \\ \alpha_x \\ \alpha_y \end{vmatrix}_{(i)} - \left[J\right]^{-1}_{(i)} \begin{vmatrix} R_o \\ R_x \\ R_y \end{vmatrix}_{(i)} \qquad (13)$$

where $J$ is the symmetric Jacobian matrix

$$J = \begin{bmatrix} k & m_x & -m_y \\ m_x & K_x & -K_{xy} \\ -m_y & -K_{xy} & K_y \end{bmatrix} \qquad (14)$$

in which the residual vector is

$$\begin{vmatrix} R_o \\ R_x \\ R_y \end{vmatrix}_{(i)} = \begin{vmatrix} F \\ G \\ H \end{vmatrix}_{(i)} + \begin{vmatrix} -P \\ -M_x - Py_p \\ -M_y + Px_p \end{vmatrix}_{(i)}$$

and F, G, and H are the first terms in eqs. (9), (10) and (11) respectively. Also,

$$k = \sum_{j=1}^{2} \frac{1}{t_j} \int_{A_j} E_j(x,y)\, dA \; ; \; m_x = \sum_{j=1}^{2} \frac{1}{t_j} \int_{A_j} y E_j(x,y)\, dA \; ; \; m_y = \sum_{j=1}^{2} \frac{1}{t_j} \int_{A_j} x E_j(x,y)\, dA$$

$$K_x = \sum_{j=1}^{2} \frac{1}{t_j} \int_{A_j} y^2 E_j(x,y)\, dA \; ; \; K_y = \sum_{j=1}^{2} \frac{1}{t_j} \int_{A_j} x^2 E_j(x,y)\, dA \; ; \; K_{xy} = \sum_{j=1}^{2} \frac{1}{t_j} \int_{A_j} xy E_j(x,y)\, dA$$

and $E_1(x,y)$ and $E_2(x,y)$ are the filler bar and SIP tangent stiffnesses respectively which may be found by differentiating eq. (4) to give

$$E_j(x,y) = \frac{\partial \sigma_j}{\partial \epsilon_j}$$

In order to provide the initial values of $W_o$, $\alpha_x$, and $\alpha_y$ when $i = 1$ in eq. (13), the following procedure commonly employed in such nonlinear problems is used. First, $P$, $M_x$, and $M_y$ in eqs. (9) - (11) are replaced by $\lambda P$, $\lambda M_x$, and $\lambda M_y$ respectively. The load parameter, $\lambda$, is then incremented from 0 to 1 in prescribed steps. At $\lambda = 0$, the iterations of eq. (13) are initiated using $W_o = \alpha_x = \alpha_y = 0$ as trail values, and the iterations are allowed to converge. (These trial values are the exact solutions when no mismatch or substrate deformation is present; $\bar{w} = 0$). At each succeeding value of $\lambda$, the iteration procedure of eq. (13) is carried out using the converged solution at the preceeding value of $\lambda$ as the initial trail solution.

## Uniqueness of Solution

It is shown in this section that for each set of prescribed stress-strain relationships governing the nonlinear SIP and filler bar behavior, only one solution of the equilibrium equations, eq. (1) - (3), exists independent of the order in which loads and/or substrate deformations are applied. To this end, the determinant of J is considered.

Expanding eq. (14) gives

$$|J| = k K_x K_y + 2 m_x m_y K_{xy} - m_x^2 K_y - m_y^2 K_x - k K_{xy}^2$$

Since the axis system used for evaluating the eqs. (1) - (3) is arbitrary, a set of axes $\hat{x} - \hat{y}$ may be sought about which

$$m_x = m_y = K_{xy} = 0$$

The origin of this axis system $x_o, y_o$ relative to the $x - y$ axes is given by

$$x_o = \frac{1}{k}\sum_{j=1}^{2} \frac{1}{t_j}\int_{A_j} x E_j(x,y)\, dA$$

$$y_o = \frac{1}{k}\sum_{j=1}^{2} \frac{1}{t_j}\int_{A_j} y E_j(x,y)\, dA$$

and its angular orientation, $\beta$, relative to the $x - y$ axes is

$$\beta = \frac{1}{2}\tan^{-1}\left(\frac{2 K_{xy}}{K_x - K_y}\right)$$

In the $\hat{x} - \hat{y}$ coordinate system,

$$|J| = k K_{\hat{x}} K_{\hat{y}}$$

The SIP and filler bar stress-strain relationships can be constructed such that $E_j(x,y)$ is unique and positive, hence,

$$|J| > 0$$

Consider next the schematic load deflection curves in figure 7. If the dashed secondary solution curve exists, it must be a branch of the primary curve inasmuch as all solutions must yield zero load at zero deflection. However, since $|J| \neq 0$, there cannot be a branch (or bifurcation) point, and hence, only the primary solution exists. Consequently, once a set of stress-strain relationships for the SIP and filler bar are chosen, the solutions are unique independent of

the order of load and/or substrate deformation application. However, to the extent that the selection of the stress-strain relation depends on load history, the solutions will be load history dependent.

Furthermore, since $|J|$ is always positive, Newton's iteration should converge for sufficiently small increments in $\lambda$ . Experience indicates that $\lambda$ increments of 0.1 are in most cases sufficient.

## DISCUSSION OF RESULTS

### Parametric Studies on Square Tiles

A large number of tiles are of square planform with nominal dimensions of 6" x 6" on a 5" x 5" SIP footprint. For the purpose of examining trends arising from parametric studies, it is useful to consider such tiles. (An actual tile of odd shape is considered at the end of this section).

Effect of mismatch at different shock levels - Figure 2 presents the linear and nonlinear predicted maximum through-the-thickness SIP/RSI interface stress levels under a simulated transonic shock condition on a 3.81 cm (1.5 in) thick tile using Rockwell generated stress-strain data corresponding to 50 load cycles at $\pm$68.95 kPa ($\pm$10 psi) as given in ref. 1. (The effect of other stress-strain data is considered later in this section). The tile is considered with and without a spherical mismatch of .048 cm (.019 in.) amplitude. Since the tile is considered rigid, the shock condition is statically equivalent to a combined load-moment condition or an eccentric load condition.

The study indicates that under no external load, $\Delta p=0$, the linear solution predicts higher stresses than the nonlinear analysis when mismatch is present. This is due to the very low stiffness (about 27.58 kPa or 4 psi) at or near zero load, associated with the nonlinear stress-strain data, while the linear solution uses a constant 172.4 kPa (25 psi) stiffness. However, as the shock amplitude is increased, the situation reverses and the nonlinear solution predicts considerably higher stresses than the linear solution; when $\Delta p \gtrsim$ 4.8 kPa (0.7 psi) the linear solution being up to 43% lower (nonconservative). The same tile without mismatch shows that the linear analysis is always nonconservative. Although not shown, these trends exhibited here are generally true for other loading conditions. Thus, due to the nonlinear SIP behavior, caution must be exercised in assessing the effect of mismatch, since as is shown, its affect varies with load level.

It is also of interest to consider the distribution of the SIP/RSI through-the-thickness interface stresses. This is shown in figure 3. The figure shows that due to the low stiffness of the SIP at small strains, the majority of the tile carries relatively little stress, while the edges of the interface carry a highly concentrated stress.

Effect of Filler Bar - Figure 4 shows the effect of different filler bar dimensions on the predicted nonlinear interface stresses for a square tile under combined load and moments. In this study, the SIP footprint dimensions are fixed to be 12.7 x 12.7 $cm^2$ (5 x 5 $in^2$) and the surrounding filler bar dimension is increased from $\ell_f$ = 0 to 3.81 cm (1.5 in). Maximum interface stresses for different combinations of load and moment are presented as ratios to the corresponding linear solution without filler bar, which is the value that the present Rockwell procedure would give for the same load and moment. Since the filler bar is only effective in compression, a moment must be applied to work the filler bar. For the study presented here that moment, M, was fixed at 16.9 N·m (150 lb.·in.) and a direct tensile load, P, of variable magnitude was assumed to act simultaneously.

The figure indicates that the nonlinear solution without filler bar $\ell_f$ = 0, is up to 70% higher than the RI solution and decreases with increasing $\ell_f$, in a nearly linear fashion for all values of P. As the load P is increased, the tile will be pulled further off of the filler bar which is only effective in compression and, hence, the effect of the filler bar is decreased and the curves tend to become horizontal as the figure shows. However, for the nominal filler bar dimension used in the actual tiles, $\ell_f \leq$ 1.27 cm (0.5 in), the presence of the filler bar is not sufficient to reduce the maximum stresses to the linear analysis value; the stresses still being 10 to 30% higher than the RI solution when $\ell_f$ = 1.27 cm (0.5 in).

Effect of Different Stress-Strain Data - As a consequence of the preceding discussion, it is clear that the linear solution may yield nonconservative results. However, as observed by others, the stress-strain behavior is strongly history dependent and exhibits considerable scatter from one specimen to another. The natural desire is to choose the stress-strain data giving the worst or most critical situation, however, this cannot be done without first examining the effect of the different stress-strain data. The purpose of this section is to pursue this examination on a square tile under shock loading. The stress-strain

data considered were generated by Rockwell and are as follows:

(1) 2nd cycle data to ±68.95 kPa (±10 psi); denoted as RI2

(2) 50th cycle data to ±68.95 kPa (±10 psi); denoted as RI50

(3) 90% Max data; denoted as RI90MAX

(4) Average data; denoted as RIAV

where (1) and (2) are given in reference 1, and (3) and (4) are given in reference 2. For all data, the stress-strain curves are linearly extrapolated above the strain levels for which the data are valid.

A comparison of the results shown in figure 5 reveals a relatively wide variation when different stress-strain data is used in the presence of mismatch, however, the trends discussed previously for the RI50 data remain unchanged. It may be argued that the RI50 results are too conservative since their use implies that the tile has seen 50 cycles at 68.95 kPa (±10 psi) which is quite high. In fact, high stress cycles tend to increase the deadband which, in turn, produces higher stress concentrations at tile corners while cycles at lower stress levels do little to extend the deadband. Therefore, the RI2 curve is probably more reasonable.

## Outboard Elevon Trailing Edge Upper Surface Tile

In addition to the parametric studies described previously, the analysis has also been applied to the outboard elevon trailing edge upper surface tile, #139, as shown in figure 6 for descent at +20° flap using RI2 data extended to ±103.4 kPa (±15 psi) from curve 6M2A of ref. 3. The figure illustrates the highly nonlinear interface stress distribution predicted on such an odd shaped tile under the expected load and moments. For the purpose of comparing the linear and nonlinear solutions, a linear solution without filler bar was used since this corresponds to the Rockwell analysis procedure.

From the figure it is observed that the maximum nonlinear stress when filler bar is absent is about 53% larger than the maximum linear stress. When filler bar is added, this percentage decreases slightly to 49%. The addition of the filler bar helps to distribute the compressive stresses so that these are highly reduced, but has little effect in reducing the tensile stresses.

## CONCLUSIONS

A nonlinear analysis has been developed to predict the SIP/RSI through-the-thickness interface stresses including the effects of mismatch and filler bar. The analysis assumes that the tile is rigid and the SIP and filler bar behave as a nonlinear spring foundation which is characterized by experimental stress-strain data. Interface stresses are calculated numerically from the equilibrium of the tile using a Newton iteration scheme.

As a result of parametric studies for a simulated shock loading on square tiles, the following conclusions are derived:

1. When no mismatch is present, linear solutions for maximum interface stresses tend to be nonconservative relative to nonlinear solutions.
2. When mismatch is present, linear solution relative to nonlinear solutions tend to be only conservative at low load levels and become highly nonconservative at higher levels.
3. Use of filler bar reduces no. linear stresses, but for nominal dimension filler bar up to 1.27 cm (½") wide, reductions are generally small, thus linear analysis without filler bar as used by Rockwell still underestimates the nonlinear analysis with filler bar.
4. Conclusions 1, 2, and 3 are generally independent of the choice of different Rockwell stress-strain data; however, the magnitude of the difference between linear and nonlinear solutions can vary significantly when large mismatches are present.

The analysis has also been applied to the outboard trailing edge elevon tile, (tile 139), for descent at $+20^{\circ}$ flap. Results for this tile indicate that the linear analysis underestimates the maximum interface stress by 49% even when filler bar is present.

## REFERENCES

1. Load Versus Deflection Characteristics of SIP; Interim Report No. 2, LTR 2345-4201; Rockwell International, Shuttle Orbiter Division, September 29, 1978; Appendix A, pg. 65.

2. Material Properties Manual; Vol. 3; Rockwell International, Shuttle Orbiter Division, May 1979.

3. Load Versus Deflection Characteristics of SIP; Interim Report No. 2, LTR 2345-4203, Rockwell International, Shuttle Orbiter Division, October 1978, Appendix D, pg. 43.

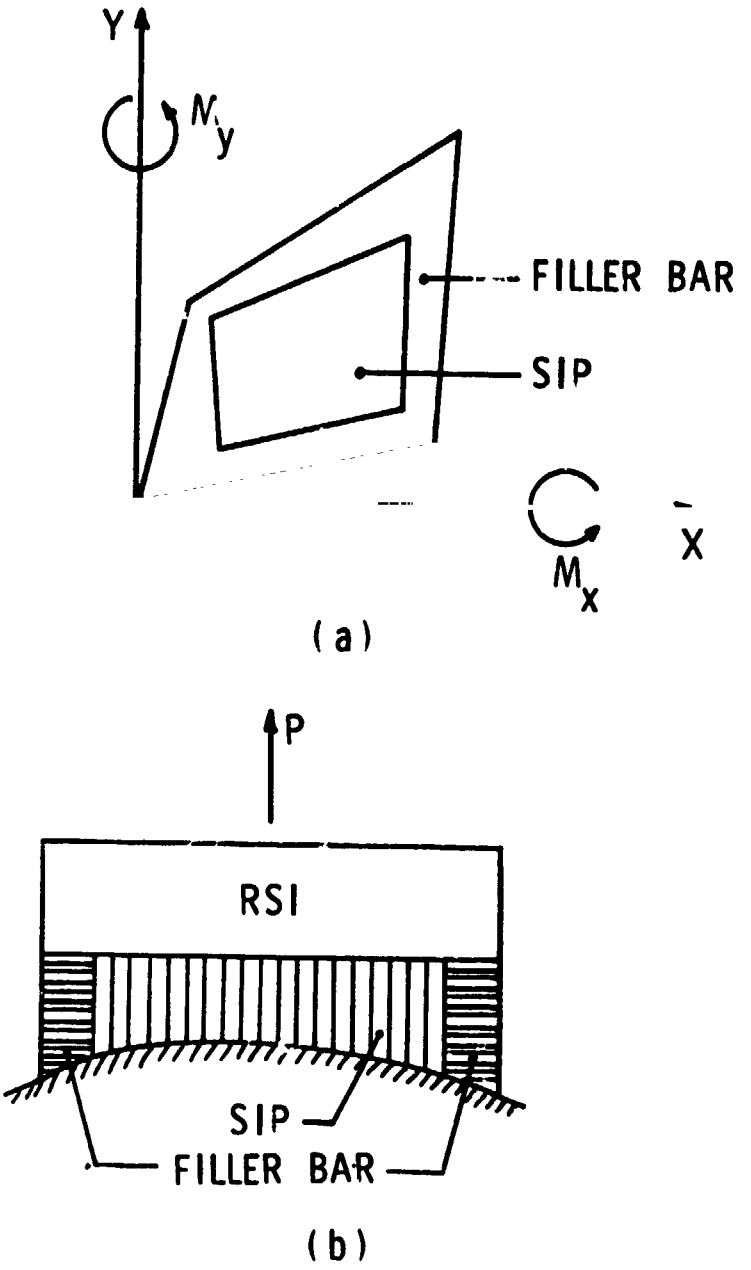


Figure 1. TPS Geometry:
(a) SIP footprint and filler bar planform
(b) RSI tile profile

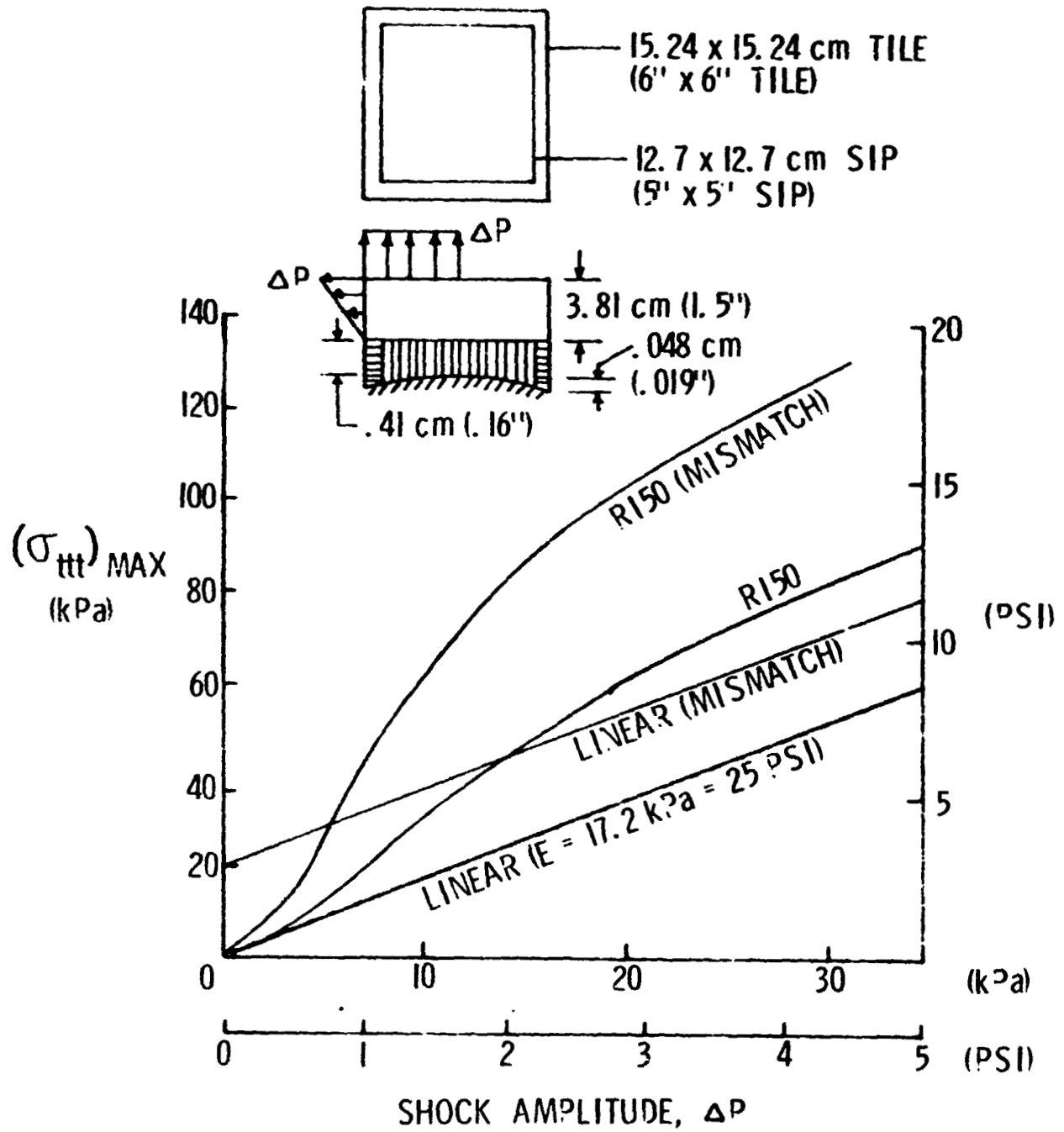


Figure 2. Variation of maximum interface stress with simulated shock magnitude for a square tile with and without spherical mismatch.

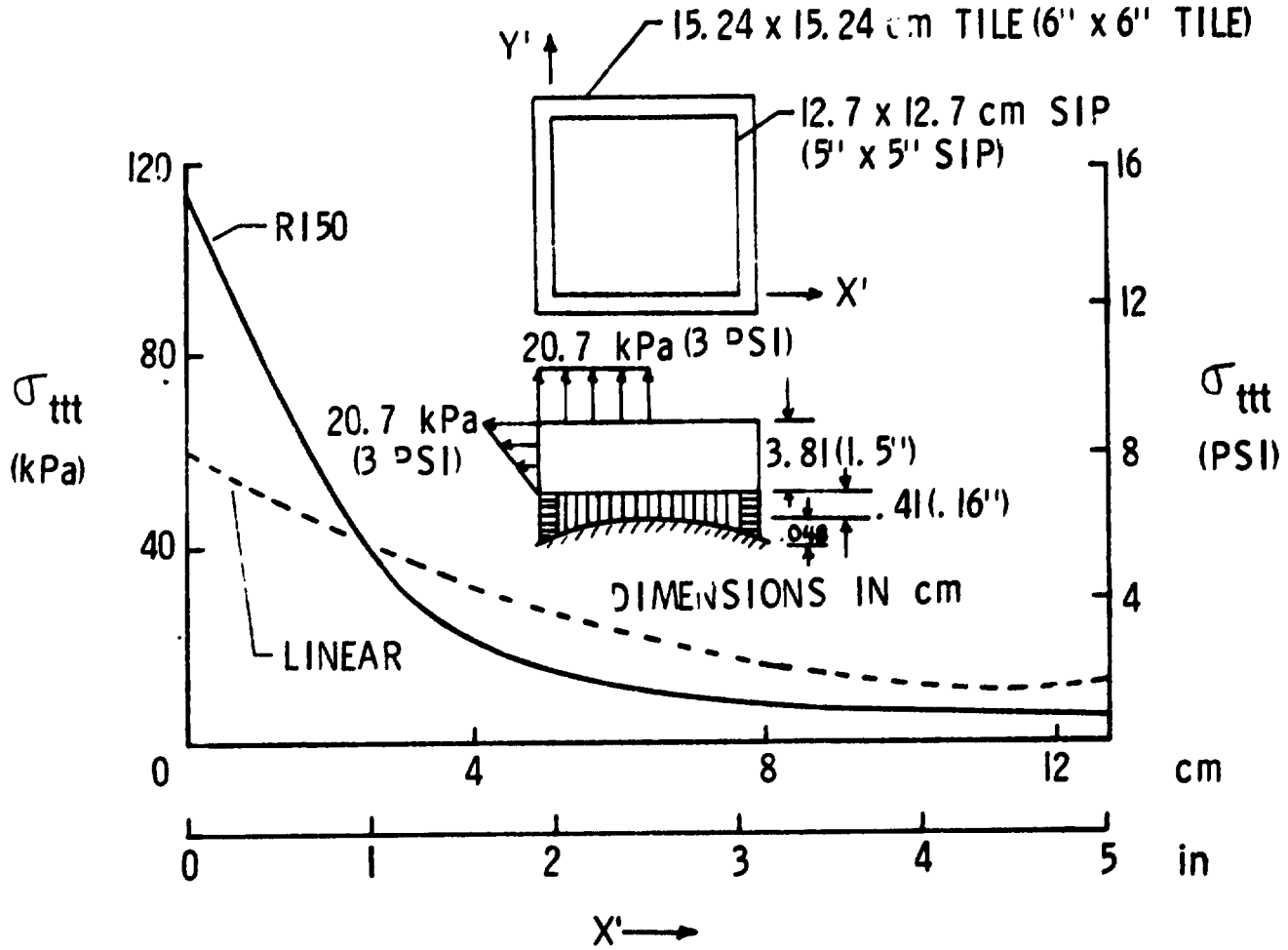


Figure 3. Variation of through-the-thickness SIP/RSI Interface Stress at y'=0 for 20.7 kPa (3 PSI) Simulated Transonic Shock for RI50 and Linear (E=17.2 kPa=25 PSI) SIP on Tile with Spherical Mismatch.

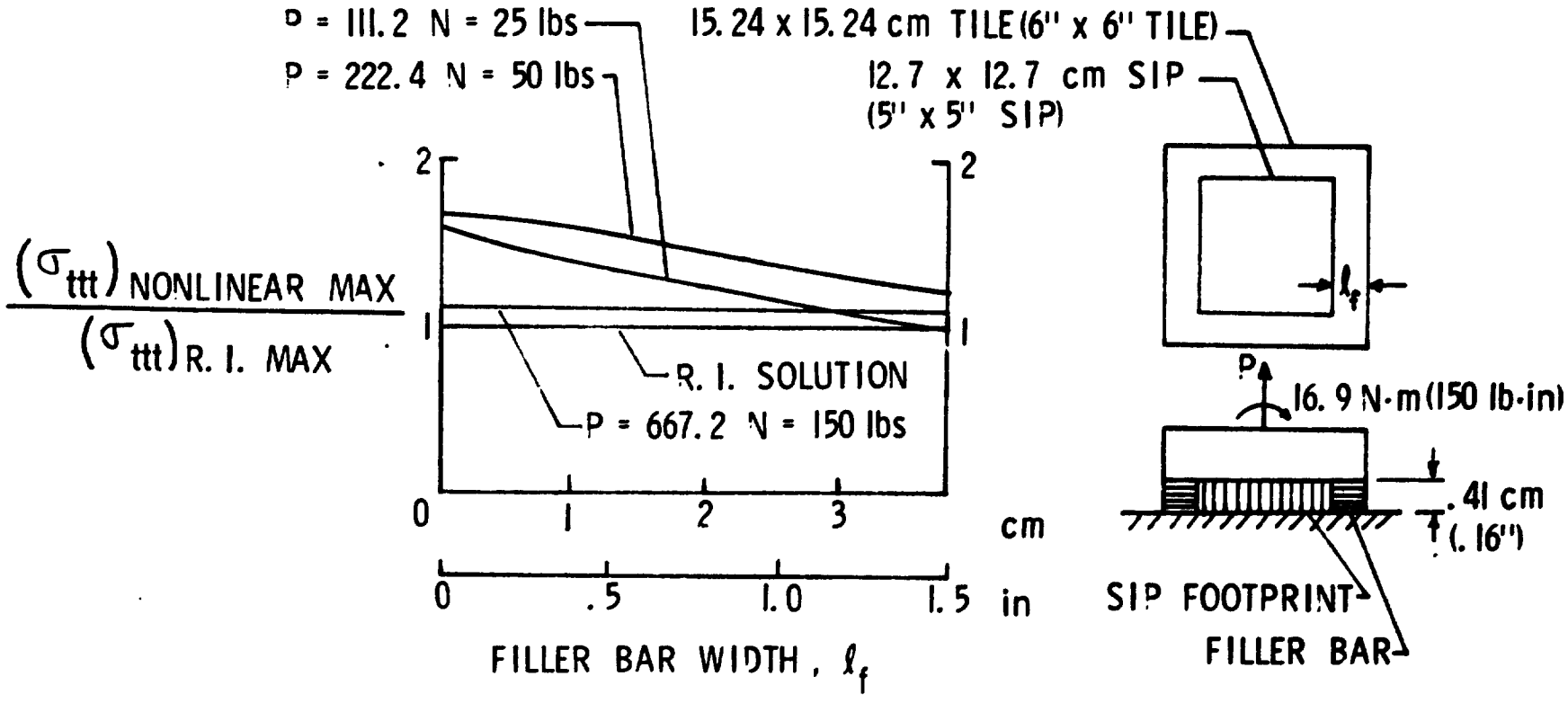


Figure 4. Effect of different filler bar widths on the maximum interface stress in square tiles under combined load and moment.

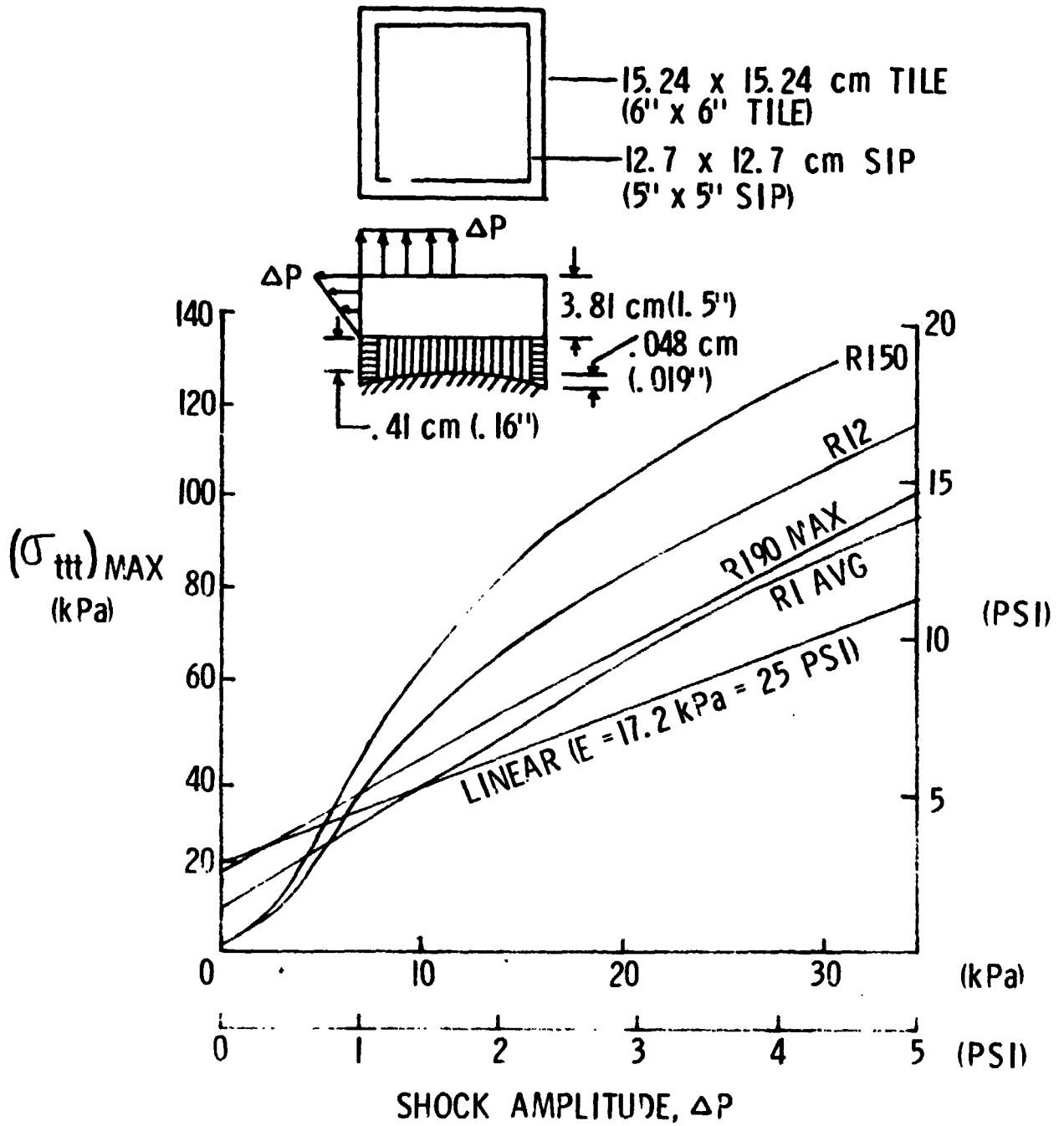


Figure 5. Effect of Different Stress-Strain Data on Maximum Through-the-Thickness SIP/RSI Interface Stress for Shock on Square Tile With Spherical Mismatch

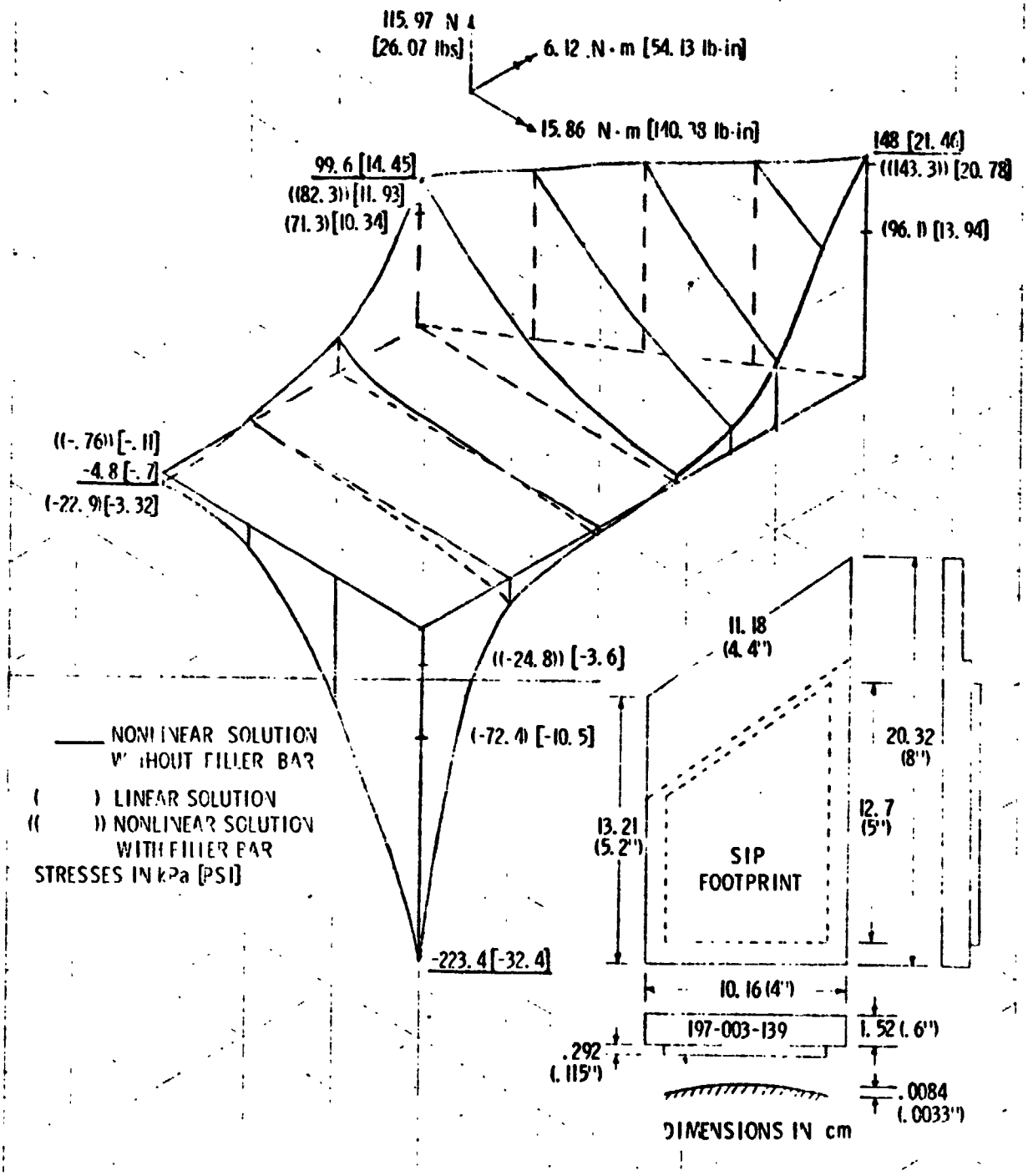


FIGURE 6. LINEAR & NONLINEAR 2-D PREDICTED SIP-RSI INTERFACE STRESSES IN OUTBOARD ELEVON TRAILING EDGE UPPER SURFACE TILE - LOAD CASE: DESCENT 20° FLAP

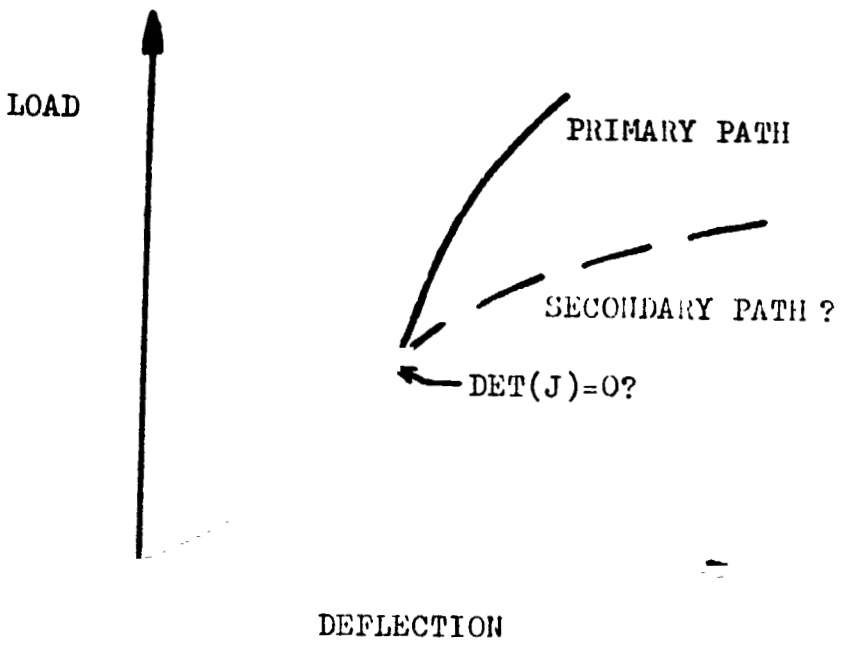


**Figure 7. Schematic of possible load-deflection paths**